Inorg. Chem. **2004**, *43*, 3377–3385

Synthesis and Properties of Dimetallic M^1[Pz]–M^2[Schiff Base] Complexes

Min Zhao,[†] Chang Zhong,[†] Charlotte Stern,[†] Anthony G. M. Barrett,*[,‡] and Brian M. Hoffman*[,†]

Departments of Chemistry, Northwestern University, Evanston, Illinois 60208-3113, and Imperial College of Science, Technology, & Medicine, London SW7 2AY, U.K.

Received December 5, 2003

We report the synthesis and physical characterization of a series of peripherally functionalized porphyrazines (pz's) **1**[M^1; M^2; R], where M^1 is a metal ion incorporated into the pz core, M^2 is a metal ion bound to a bis(5-*tert*-butylsalicylidenimine) chelate built onto two amino nitrogen attached to the pz periphery, and R is a solubilizing group (either *n*-propyl (Pr) or 3,4,5-trimethoxyphenyl (TMP) group) attached to the remaining carbons of the pz periphery. The **1**[M^1; M^2; R] species are prepared from precursor pz's with a selenodiazole ring; they are deprotected to form the diamino pz, which reacts with two moles of 5-*tert*-butyl-2-hydroxybenzaldehyde to form the Schiff base pz. This is metalated to form **1**[M^1; M^2; R]. The crystal structures of **1**[2H; Ni; Pr] and **1**[Cu; ClMn; Pr] are presented. The EPR spectra of the M^1–M^2 "isomers" prepared with Cu(II) ($S = {}^1/_2$) and ClMn(III) ($S = 2$) ions, **1**[ClMn; Cu; Pr] and **1**[Cu; ClMn; TMP], are a superposition of spectra expected for the $S = {}^3/_2$ and $S = {}^5/_2$ total-spin manifolds that result from strong Heisenberg coupling between the partner spins. The exchange splitting between the two manifolds, as determined by temperature-dependent magnetic susceptibility measurements, is equivalent for the two M^1–M^2 "isomers", $\Delta/k_B \approx 20$–25 K, which suggests a σ-pathway for exchange coupling.

Introduction

Ligand systems capable of binding multiple metal ions are of great interest because their metal complexes have applications that include electron transfer,[1] macrocycle mediated spin coupling,[2,3] ultra-high-spin molecules,[4] and biomimetic chemistry.[5] We have shown that porphyrazine (pz) macrocycles can template the rigid organization of multiple metal centers through application of procedures developed for synthesizing porphyrazines of the form M[Pz($\mathbf{A}_n$; $\mathbf{B}_{4-n}$)], $n = 1$, 2, 3, and 4. The **A** groups are designed to introduce a novel "chemistry", including exocyclic metal-ion binding; the **B** groups can contribute to the electronic, optical, or redox properties but typically are chosen so as to optimize the yield for a desired *n* and/or geometry and to confer proper solubility. In this way, porphyrazines have been prepared in which exocyclic metal ions bind to sulfur,[6−8] nitrogen,[9,10] or oxygen[11] atoms attached to the macrocycle periphery. Such multimetallic systems have the potential to exhibit electron transfer or magnetic exchange between metal ions, as illustrated by the core-periphery spin coupling seen when a metal ion is bound to a peripheral dithiolene.[8,9,12]

The recent synthesis of a ClMn[Pz(**A**; $\mathbf{B}_3$)] pz where **A** is a Cu Schiff base unit appended to the periphery and **B** is

* To whom correspondence should be addressed. E-mail: bmh@northwestern.edu (B.M.H.); agmb@ic.ac.uk (A.G.M.B.).
† Northwestern University.
‡ Imperial College of Science, Technology, & Medicine.

(1) *Electron Transfer and Radical Processes in Transition Metal Chemistry*; Astruc, D., Ed.; VCH Publishers: New York, 1995.
(2) Kahn, O. *Molecular Magnetism*; VCH Publishers: New York, 1993.
(3) Attia, A. S.; Conklin, B. J.; Lange, C. W.; Pierpont, C. G. *Inorg. Chem.* **1996**, *35*, 1033−1038.
(4) Goldberg, D. P.; Koulougliotis, D.; Brudvig, G. W.; Lippard, S. J. *J. Am. Chem. Soc.* **1995**, *117*, 3134−3144.
(5) Sessler, J. I.; Sibert, J. W.; Lynch, V.; Markert, J. T.; Wooten, C. I. *Inorg. Chem.* **1993**, *32*, 621−626.
(6) Velázquez, C. S.; Fox, G. A.; Broderick, W. E.; Andersen, K. A.; Anderson, O. P.; Barrett, A. G. M.; Hoffman, B. M. *J. Am. Chem. Soc.* **1992**, *114*, 7416−7424.
(7) Baumann, T. F.; Nasir, M. S.; Sibert, J. W.; White, A. J. P.; Olmstead, M. M.; Williams, D. J.; Barrett, A. G. M.; Hoffman, B. M. *J. Am. Chem. Soc.* **1996**, *118*, 10479−10486.
(8) Michel, S. L. J.; Goldberg, D. P.; Stern, C. L.; Barrett, A. G. M.; Hoffman, B. *J. Am. Chem. Soc.* **2001**, *123*, 4741−4748.
(9) Goldberg, D. P.; Montalban, A. G.; White, A. J. P.; Williams, D. J.; Barrett, A. G. M.; Hoffman, B. M. *Inorg. Chem.* **1998**, *37*, 2873−2879.
(10) Lange, S. J.; Nie, H.; Stern, C. L.; Barrett, A. G. M.; Hoffman, B. M. *Inorg. Chem.* **1998**, *37*, 6435−6443.
(11) Cook, A. S.; Williams, D. B. G.; White, A. J. P.; Williams, D. J.; Lange, S. J.; Barrett, A. G. M.; Hoffman, B. M. *Angew. Chem., Int. Ed. Engl.* **1997**, *36*, 760−761.
(12) Michel, S. L. J.; Baum, S.; Barrett, A. G. M.; Hoffman, B. M. *Prog. Inorg. Chem.* **2001**, *50*, 473−590.

10.1021/ic035402x CCC: $27.50
Published on Web 05/06/2004

Table 1. M^1[Pz]−M^2[Schiff Base] Complexes Prepared

1[M^1; M^2; R]	S_1	S_2	S^a	zfs (cm^{-1})	$J/k_B{}^d$ (K)	A (G)	scheme
1[2H; Ni; Pr]	0	0	0				1
1[Ni; Ni; Pr]	0	0	0				1,2
1[ClMn; Ni; Pr]	2	0	2	$D^{Mn} = -2.3^b$			2
1[ClMn; Cu; Pr]	2	1/2	3/2	$D^{Mn} = -2.3^b$	4.6	$A_{Mn}{}^{5/2} = 53^e$	1,2
			5/2			$A_{Mn}{}^{3/2} = 80^e$	
1[Cu; ClMn; Pr]	1/2	2	3/2	$\{D_{Mn} = -2.47 \pm 0.02^c\}$	4.1		2
			5/2	$\{\lvert E_{Mn}\rvert = 0.17 \pm 0.01\}$			
1[Cu; ClMn; TMP]	1/2	2	3/2	$\{D^{Mn} = -2.47 \pm 0.02^c\}$	4.1	$A_{Mn}{}^{5/2} = 55^f$	2
			5/2	$\{\lvert E_{Mn}\rvert = 0.17 \pm 0.01\}$		$A_{Mn}{}^{5/2} = 82.5^f$	

[a] Expected total-spin generated from strong exchange coupling between two individual spins. [b] Reference 30. [c] Reference 31. [d] Calculated from experimental data. [e] Experimental data. [f] Simulated data.

Chart 1

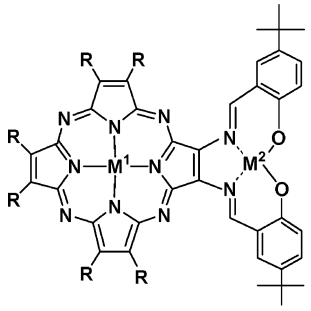

1[M^1; M^2; R]

two *n*-propyl groups (Chart 1) further showed that amino-functionalized pz's can act as scaffolds on which to erect complex chelates for the preparation of multimetallic pz's. This complex displays Heisenberg exchange between the core Mn(III) ion ($S = 2$) and peripheral Cu(II) ion ($S = {}^1/_2$) that leads to states of total spin $S = {}^5/_2$, ${}^3/_2$ in thermal equilibrium.[13] For simplicity here, we shall denote this compound as **1**[M^1; M^2; R], where M^1 = ClMn, M^2 = Cu, and R = Pr (Chart 1).

In the preparation of high-spin multimetallic pz's, it is desirable to have high-spin metal ions on the periphery and an ion with $S = {}^1/_2$ in the core, and not the reverse: with *n* peripheral ions of S_2, antiferromagnetic periphery-core coupling will give a "ferrimagnetic" complex where the peripheral spins align antiferromagnetically with the core spin, and where the ground state has $S = n[S_2 - {}^1/_2]$. Hence, from this perspective, the metalation pattern of the compound **1**[ClMn; Cu; Pr] is "backward". We thus have devised procedures that allow us to "switch" the two metal ions. This effort includes the development of alternate synthetic routes that optimize the selectivity and yield in the formation of mixed-metal Schiff base pz's. In addition, we have developed a new **B**, bis(3,4,5-trimethoxyphenyl), (bis(TMP)), designed to enhance the solubility of the multimetallic complexes. Using these procedures, we have prepared and characterized the dimetallic Schiff base pz's, **1**[M^1; M^2; R], listed in Table 1. The results reported here begin the effort to define the systematics of spin coupling within the Schiff base pz system with the determination of exchange parameters for the two M^1−M^2 "isomers" prepared with Cu(II) ($S = {}^1/_2$) and ClMn(III) ($S = 2$) ions.

(13) Zhao, M.; Stern, C.; Barrett, A. G. M.; Hoffman, B. M. *Angew. Chem., Int. Ed.* **2003**, *42*, 462−465.

Experimental Section

All starting materials were purchased from Aldrich Chemical and used as received, with the exception of anhydrous $MnCl_2$, which was purchased from Alfa Aesar and used as received. All solvents were used as supplied. Anhydrous NH_3 (Linde Specialty Gases) was ultrahigh-purity grade. Sodium metal was freshly cut under hexanes prior to use. Silica gel used for chromatography was Whatman silica gel 60 Å (230−400 mesh) from VWR. Porphyrazine **4**[Pr] and **7**[Pr] were prepared as previously reported.[14] 3,4-Dicyano-1,2,5-selenodiazole (DCSD) was prepared according to the literature.[15]

^{1}H NMR spectra were obtained using a mercury 400 MHz and an Inova 500 MHz spectrometers. Electronic absorption spectra were recorded using a Hewlett-Packard HP8452A diode array spectrophotometer. Elemental analyses were performed by Quantitative Technologies Inc. (Whitehouse, NJ). Fast atom bombardment mass spectra were recorded by the Mass Spectrometry Laboratory of the University of Illinois at Urbana Champaign. Atmospheric-phase chemical ionization mass spectra and electrospray ionization mass spectra were recorded locally using a Micromass Quattro II RCMS triple-quadrupole instrument. Cyclic voltammetry experiments were done at room temperature in methylene chloride with 0.1 M tetrabutylammonium hexafluorophosphate as the supporting electrolyte using a Cypress Systems 2000 electroanalytical system. A platinum working electrode, a Ag/AgCl reference electrode, and a Ag wire counter electrode were used, with ferrocene (Fc) added to the cell at the end of the experiment as an internal reference. All $E_{1/2}$ values were calculated from $(E_{pa} + E_{pc})/2$ at a scan rate of 110 mV s^{-1} and no correction for junction potentials. Electron paramagnetic resonance (EPR) spectra were measured by using a modified Varian E-4 X-band spectrometer. Solid-state magnetic susceptibility measurements were made by using a Quantum Design MPMS SQUID susceptometer operating in the temperature range 2−300 K and equipped with a 500 G field.

Bis(3,4,5-trimethoxyphenyl)fumaronitrile, 2. Fresh cut Na (7.30 g, 0.317 mol) was added to MeOH (80 mL) cooled to 0 °C. The sodium methoxide was added dropwise over 0.5 h to a solution of 3,4,5-trimethoxyphenylacetonitril (30.0 g, 0.145 mol) and I_2 (36.78 g, 0.145 mol) dissolved in diethyl ether (500 mL) at 0 °C. The dark brown color of the solution cleared, and a yellow precipitate formed, which was collected, washed with cold MeOH, and dried under vacuum. The filtrate volume was reduced by half

(14) Baum, S. M.; Trabanco, A. A.; Andres, A.; Montalban, A.; Micallef, A. S.; Zhong, C.; Meunier, H. G.; Suhling, K.; Phillips, D.; White, A. J. P.; Williams, D. J.; Barrett, A. G. M.; Hoffman, B. M. *J. Org. Chem.* **2003**, *68*, 1665−1670.

(15) Bauer, E. M.; Ercolani, C.; Galli, P.; Popkova, I. A.; Stuzhin, P. A. *J. Porphyrins Phthalocyanines* **1999**, *3*, 371−379.

and was placed in freezer overnight. A second crop of product was filtered out, washed, and dried under vacuum. Total yield: 22.6 g, 76.9%. ^{1}H NMR (400 MHz, $CDCl_3$) δ 3.95 (12H, s), 3.96 (6H, s), 7.08 (4H, s). EI-MS *m*/*z*: 410.1 $(M)^+$, calcd $C_{22}H_{22}N_2O_6$ 410.1.

3,4-Bis(3,4,5-trimethoxyphenyl)pyrroline-2,5-diimine, 3. Compound **2** (15.80 g, 0.03854 mol) was suspended in *n*-propanol (500 mL) and heated to reflux. Small chunks of Na (∼100 mg) were added to the reaction. Gaseous NH_3 was bubbled through the suspension. After 4 h, the solution was filtered hot, and the filtrate volume was reduced to 100 mL and poured into ice. A greenish yellow precipitate was collected by filtration and washed with water. The solid was then washed with methanol until the washes were colorless. The methanol filtrate was then evaporated, and the residue was applied to a column for chromatography with 3% methanol in methylene chloride. Compound **3** was separated as a greenish yellow powder. Total yield: 9.868 g, 59.94%. ^{1}H NMR (400 MHz, $CDCl_3$) δ 3.73 (12H, s), 3.86 (6H, s), 6.49 (4H, s). ESI-MS *m*/*z*: 428.7 $(M + H)^+$, calcd $C_{22}H_{26}N_3O_6$ 428.2.

Mg[Pz(A;B$_3$)], A = Selenodiazole, B = (3,4,5-Trimethoxyphenyl)$_2$, 4[TMP]. Magnesium metal (∼100 mg) and 50 mL of *n*-propanol were heated to reflux under N_2, and a small amount of I_2 was added to help the formation of $Mg(OPr)_2$. After 12 h, 772.0 mg (1.643 mmol) of **3** and 300.6 mg (1.643 mmol) of DCSD were added. The reaction was heated at reflux for 12 h more. The *n*-propanol was removed under vacuum. Column chromatography with 4% methanol in chloroform as eluant was performed to get the pure magnesium form of the pz, 110.0 mg (yield 13.96%). UV−vis (CH_2Cl_2) λ_{max} 362, 617, 689. ^{1}H NMR (400 MHz, $CDCl_3$) δ 3.56−3.69 (24H, m), 4.02 (12H, s), 4.08 (6H, s), 4.10−4.14 (12H, m), 7.01 (2H, s), 7.08 (2H, s), 7.48 (4H, s), 7.80 (2H, s), 7.99 (2H, s). ESI-MS *m*/*z*: 1439.4 $(M + H)^+$, calcd $C_{70}H_{67}N_{10}O_{18}MgSe$ 1439.6.

H$_2$[Pz(A;B$_3$)], A = Selenodiazole, B = (3,4,5-Trimethoxyphenyl)$_2$, 7[TMP]. Compound **4**[TMP] (90.5 mg, 0.0629 mmol) was treated with trifluoroacetic acid in the dark. After 10 min, the solution was poured over ice. Ammonium hydroxide was added to neutralize the solution. A purple precipitate was collected by filtration, washed with water, and dried under vacuum. Yield 80.0 mg, 89.7%. UV−vis (CH_2Cl_2) λ_{max} 342, 535, 579, 710. ^{1}H NMR (400 MHz, $CDCl_3$) δ 3.60 (12H, s), 3.62 (12H, s), 4.03 (12H, s), 4.09 (6H, s), 4.11 (6H, s), 4.13 (6H, s), 7.45 (4H, s), 7.58 (4H, s), 7.84 (4H, s). APCI-MS *m*/*z*: 1417.4 $(M + H)^+$, calcd $C_{70}H_{69}N_{10}O_{18}Se$ 1417.4.

General Procedures to Synthesize M[Pz(A;B$_3$)], A = Selenodiazole, B = (*n*-Propyl)$_2$ or (3,4,5-Trimethoxyphenyl)$_2$, 8[M¹; R]. To the solution of **7**[R] in DMF/chlorobenzene (4:1) was added 10-fold excess M^1X_2. The reaction mixture was stirred at 100 °C for 2−5 h. During this time, the characteristic spectrum of the porphyrazine in free base form changed completely to that of the metalated product. The solvents was rotary evaporated, and the residues were washed by methanol. **8**[Ni; Pr] yield: 90.1%. UV−vis (CH_2Cl_2) λ_{max} (log ϵ) 332 (4.51), 346 (4.51), 578 (4.36), 634 (4.37). ^{1}H NMR (400 MHz, $CDCl_3$) δ 1.10−1.18 (18H, m), 1.59−1.65 (4H, m), 2.05−2.14 (8H, m), 3.59 (4H, t, J = 19 Hz) 3.63−3.72 (8H, m). FAB-MS *m*/*z*: 728$(M)^+$, calcd $C_{34}H_{42}N_{10}SeNi$ 728. **8**[Cu; Pr] yield: 84.9%. UV−vis (CH_2Cl_2) λ_{max} (log ϵ) 339 (4.58), 354 (4.63), 581 (4.41), 593 (4.42), 636 (4.50). FAB-MS *m*/*z*: 734 $(M + H^+)$, calcd $C_{34}H_{43}N_{10}SeCu$ 734. **8**[Cu; TMP] yield: 94.2%. UV−vis (CH_2Cl_2) λ_{max} 342, 456, 550, 616, 685. ESI-MS *m*/*z*: 1478.3 $(M + H)^+$, calcd $C_{70}H_{67}N_{10}O_{18}CuSe$ 1478.3.

ClMn[Pz(A;B$_3$)], A = Selenodiazole, B = (*n*-Propyl)$_2$, 8[ClMn; Pr]. Compound **7**[Pr] (90.0 mg, 0.134 mmol) was dissolved in 45 mL of chlorobenzene and 15 mL of DMF, and excess $MnCl_2$ was added. The reaction was heated to 100 °C for 2 h after which time there was no free base form left. The solvents were removed under vacuum, and the residue was dissolved in methylene chloride and stirred with brine for half an hour in the air. The organic phase was then separated and chromatographed with 4% methanol in methylene chloride. Yield: 60.2 mg; 59.1%. UV−vis (CH_2Cl_2) λ_{max} 361, 618, 679. FAB-MS *m*/*z*: 725.5 $(M - Cl)^+$, calcd for $C_{34}H_{42}N_{10}SeMn$ 725.2.

H$_2$[Pz(A;B$_3$)], A = Nickel(II)-bis(5-*tert*-butyl-salicylidenimine), B = (*n*-Propyl)$_2$, 1[2H; Ni; Pr]. H_2S was bubbled through a solution of **4**[Pr] (39.4 mg, 0.0567 mmol) and 5-*tert*-butyl-2-hydroxybenzaldehyde (506 mg, 50-fold excess) in 10 mL of pyridine for 5 min, in which time the blue color changed to violet. As soon as the solvents were evaporated, the residues were prepurified via column chromatography in 4% methanol in chloroform with 0.5% triethylamine eluant, then redissolved in methanol. $NiBr_2$ (1 equiv, calcd from the starting selenodiazole porphyrazine **4**[Pr]) was then added. The reaction was allowed to stir at room temperature overnight, after which time the solvent was evaporated and the desired product was purified through column chromatography in chloroform with yield 55.0%. UV−vis (CH_2Cl_2) λ_{max} (log ϵ,) 348 (4.71), 569 (4.21), 656 (4.40), 688 (4.39). ^{1}H NMR (500 MHz, toluene, 60 °C) δ 1.08−1.18 (18H, m), 1.33 (18H, s), 1.86 (4H, q, J = 7 Hz), 2.08 (4H, q, J = 7 Hz), 2.20 (4H, q, J = 7 Hz), 3.38 (4H, t, J = 7 Hz), 3.52 (4H, t, J = 7 Hz), 3.58 (4H, t, J = 7 Hz), 7.13 (4H, s), 7.31 (2H, s), 8.99 (2H, s). APCI-MS *m*/*z*: 973 $(M + H^+)$, calcd $C_{56}H_{71}N_{10}O_2Ni$ 973.

Ni[Pz(A;B$_3$)], A = Nickel(II)-bis(5-*tert*-butyl-salicylidenimine), B = (*n*-Propyl)$_2$, 1[Ni; Ni; Pr]. There are two ways to prepare this compound. Method 1: The preparation was similar with the previous one to make **1**[2H; Ni; Pr], except that 11 equiv of $NiBr_2$ was added at the beginning. After evaporating MeOH, the reaction mixture was dissolved in 1:2 ratio DMF/chlorobenzene without purifying first, and was heated to 100 °C for 5 h. Then, the solvent was evaporated under reduced pressure. Column chromatography in chloroform gave **1**[Ni; Ni; Pr] in 33.1% yield. Method 2: H_2S were bubbled through a slurry of **8**[Ni; Pr] (18.1 mg, 0.0249 mmol) and 5-*tert*-butyl-2-hydroxybenzaldehyde (221 mg, 50-fold excess) in 20 mL of pyridine for 10 min. During this time, the solids almost dissolved. Then, the solvents were evaporated, and the residues were washed by methanol until the washes were colorless. The remaining compounds were dissolved in 1:1 ratio MeOH/$CHCl_3$, and $NiBr_2$ (5-fold excess) was added. The reaction was stirred at room temperature overnight, after which time the solvent was evaporated and column chromatography in chloroform give the desired product with yield 20.2%. UV−vis (CH_2Cl_2) λ_{max} (log ϵ) 338 (4.32), 582 (3.89), 696 (4.06). ^{1}H NMR (500 MHz, benzene, 70 °C) δ 1.05−1.15 (18H, m), 1.34 (18H, s), 1.82 (4H, q, J = 7 Hz), 2.03 (4H, q, J = 7 Hz), 2.14 (4H, q, J = 7 Hz), 3.28 (4H, s), 3.45 (4H, s), 3.53 (4H, t, J = 7 Hz), 7.16 (2H, d, J = 8 Hz), 7.24 (2H, d, J = 8 Hz), 7.32 (2H, s), 8.89 (2H, s). ^{1}H NMR (500 MHz, toluene, 60 °C) δ 0.99−1.15 (18H, m), 1.35 (18H, s), 1.86 (4H, overlapped with toluene), 2.04 (4H, q, J = 7 Hz), 2.14 (4H, q, J = 7 Hz), 3.31 (4H, t, J = 7 Hz), 3.44 (4H, t, J = 7 Hz), 3.49 (4H, t, J = 7 Hz), 7.16 (4H, s), 7.28 (2H, s), 8.81 (2H, s). FAB-MS *m*/*z*: 1029.6 $(M + H^+)$, calcd $C_{56}H_{69}N_{10}O_2Ni_2$ 1029.4.

ClMn[Pz(A;B$_3$)], A = Cu(II)-bis(5-*tert*-butyl-salicylidenimine), B = (*n*-Propyl)$_2$, 1[ClMn; Cu; Pr]. There are two ways to make this compound. Method 1: To a solution of **4**[Pr] (45.4 mg, 0.0653 mmol) and 5-*tert*-butyl-2-hydroxybenzaldehyde (583 mg, 50-fold excess) in 10 mL of pyridine was bubbled H_2S for 5 min, in which time the blue color changed to violet. As soon as the solvents were evaporated, the residues were prepurified via

column chromatography in 4% methanol in chloroform (with 0.5% triethylamine), and then dissolved in 40 mL of methanol. $CuCl_2$ (1 equiv, calcd from the starting selenodiazole porphyrazine **4**[Pr]) was then added. The reaction was allowed to stir at room temperature overnight, after which time the solvent was evaporated. A short column was applied to get rid of unreacted salts. The blue fractions were collected and dissolved in 10 mL of DMF and 20 mL of chlorobenzene. Excess $MnCl_2$ was added, and the reaction was brought to 100 °C. It was stopped when there was no change in the optical spectra. Column chromatography (10% methanol in methylene chloride) separated the green product in 30.3% yield. Method 2: Compound **8**[ClMn; Pr] (60.2 mg, 0.0792 mmol) and 5-*tert*-butyl-2-hydroxybenzaldehyde (706 mg, 3.95 mmol) were put into a three-neck round-bottom flask. Anhydrous pyridine (20 mL) was added via syringe. H_2S was bubbled through the reaction mixture for 5 min, during which time the green solution turned to purple. The solvents were evaporated under reduced pressure, and the residue was chromatographed using 4% methanol in chloroform (with 0.5% triethylamine) to get rid of most of the unreacted 5-*tert*-butyl-2-hydroxybenzaldehyde. Without further purification, the crude ligand was dissolved in 20 mL of methanol and 20 mL of chloroform and stirred with excess anhydrous $CuCl_2$ overnight. After removing the solvents, the residue was dissolved in methylene chloride, and stirred with brine for half an hour in the air. The organic phase was then separated and purified by column chromatography (10% methanol in methylene chloride). Yield: 34.5 mg, 40.9%. UV−vis (CH_2Cl_2) λ_{max} 344, 381, 656, 694. APCI-MS *m*/*z*: 1066.5 $(M + H)^+$, 1030.5 $(M - Cl)^+$, calcd $C_{56}H_{69}N_{10}O_2MnCuCl$ 1066.4, calcd $C_{56}H_{68}N_{10}O_2MnCu$ 1030.4. Anal. Calcd for $C_{56}H_{71}N_{10}O_3MnCuCl$ (**1**[ClMn; Cu; Pr] + H_2O): C, 61.98; H, 6.50; N, 12.91. Found: C, 62.01, H, 6.27; N, 13.12.

ClMn[Pz(A;B$_3$)], A = Ni(II)-bis(5-*tert*-butyl-salicylidenimine), B = (*n*-Propyl)$_2$, 1[ClMn; Ni; Pr]. This compound was prepared using method 2 for **1**[ClMn; Cu; Pr]. Yield: 46.2%. UV−vis (CH_2Cl_2) λ_{max} 367, 592, 748. ESI-MS *m*/*z* 1026.2 $(M - Cl)^+$, calcd $C_{56}H_{68}N_{10}O_2MnNi$ 1026.8. Anal. Calcd for $C_{56}H_{70}N_{10}O_3MnNiCl$ (**1**[ClMn; Cu; Pr] + H_2O): C, 62.31; H, 6.66; N, 12.57. Found: C, 62.26, H, 6.53; N, 12.97.

Cu[Pz(A;B$_3$)], A = Chloromanganese(III)-bis(5-*tert*-butyl-salicylidenimine), B = (*n*-Propyl)$_2$, 1[Cu; ClMn; Pr]. H_2S were bubbled through a slurry of **8**[Cu; Pr] (51.5 mg, 0.0703 mmol) and 5-*tert*-butyl-2-hydroxybenzaldehyde (626 mg, 50-fold excess) in 25 mL of pyridine for 10 min, in which time the solids almost dissolved. After the solvents were evaporated, the residues were washed by methanol until the washes were colorless. The remaining compounds were dissolved in EtOH/$CHCl_3$ (1:4), and 1 mL of triethylamine and anhydrous $MnCl_2$ (5-fold excess) were added. The reaction was stirred at room temperature overnight, after which time the solvent was evaporated. The residues were dissolved in CH_2Cl_2 and stirred with brine for 0.5 h in air. The organic phase was then separated, and the desired complex was purified through column chromatography in 5% MeOH in CH_2Cl_2 with yield 23.0%. UV − vis (CH_2Cl_2) λ_{max} 341, 592, 662. APCI-MS *m*/*z*: 1030.6 $(M - Cl)^+$, calcd $C_{56}H_{68}N_{10}O_2MnCu$ 1030.4. Anal. Calcd for $C_{58}H_{74}N_{10}O_3MnCuCl$ (**1**[Cu; ClMn; Pr] + EtOH): C, 62.58; H, 6.70; N, 12.58. Found: C, 63.00, H, 6.57; N, 12.12.

Cu[Pz(A;B3)], A = Chloromanganese(III)-bis(5-*tert*-butyl-salicylidenimine), B = (3,4,5-Trimethoxyphenyl)$_2$, 1[Cu; ClMn; TMP]. This compound was synthesized using the same strategy as **1**[Cu; ClMn; Pr], only NaOMe was used as the base for manganese metalation. Yield 50.2%. UV−vis (CH_2Cl_2) λ_{max} 352, 553, 660, 690. ESI-MS *m*/*z* 1775.8 $(M - Cl)^+$, calcd $C_{92}H_{92}N_{10}O_{20}MnCu$ 1776.2.

Table 2. Crystallographic Data for **1**[2H; Ni; Pr] and **1**[Cu; ClMn; Pr][a]

	1[2H; Ni; Pr]	**1**[Cu; ClMn; Pr]
formula	$C_{65.50}H_{81}O_{2.75}N_{10}Ni_{1.07}$	$C_{60}H_{74}N_{10}O_{2.5}MnCuCl$
fw	1115.15	1129.24
color, habit	opaque, needle	blue, plate
cryst size/mm^3	0.56 × 0.12 × 0.06	0.84 × 0.344 × 0.242
lattice type	triclinic	triclinic
space group, no.	$P\bar{1}$, 2	$P\bar{1}$
a/Å	10.427(2)	10.8836(17)
b/Å	14.848(3)	13.469(3)
c/Å	21.418(5)	19.382(3)
α/deg	104.000(4)	95.739(11)
β/deg	96.000(4)	96.001(10)
γ/deg	95.000(4)	95.18(2)
V/Å^3	3178.1(12)	2797.0(8)
Z	2	2
D_c/g cm^{-3}	1.154	1.343
F(000)	1169.92	1194
T/K	153	293
$2\theta_{max}$/deg	57.0	57.8
no. total reflns measured	29187	13043
no. observations	16753 ($I > 3\sigma(I)$)	8218 ($I > 2\sigma(I)$)
corrections	Lorentz-polarization SADABS absorption	
no. variables	669	678
R1[b]	0.093	0.079
wR2[c]	0.199	0.218

[a] Details in common: graphite-monochromated Mo Kα radiation, *ω* scans, Bruker SMART-1000 CCD area detector, refinement based on F^2. [b] $R1 = \sum||F_o| - |F_c||/\sum|F_o|$. [c] $wR2 = [\sum(w(F_o - F_c^2)_2)/\sum w(F_o^2)^2]^{1/2}$.

X-ray Structure Determination. A summary of the crystal data and data collection and refinement parameters for compounds **1**[2H; Ni; Pr] and **1**[Cu; ClMn; Pr] is provided in Table 2. Both structures were solved by direct methods and expanded using Fourier techniques and were refined by full-matrix least-squares based on F^2. All of the non-hydrogen atoms of both complexes were refined anisotropically. In compound **1**[2H; Ni; Pr], the solvent toluene and disordered methyl molecules were refined isotropically as was a partial nickel in the core.

Results and Discussion

Synthetic Schemes. Attempts to directly cocyclize 2,3-dipropylmaleonitrile with bis(5-*tert*-butyl-salicylidenimine)-maleonitrile or nickel(II)-bis(5-*tert*-butyl-salicylidenimine)-maleonitrile were unsuccessful. This led to the development of a scheme that involves Schiff base formation with a diamine pz. Extensive studies have been carried on pz's with peripheral dialkylamino groups,[16] generated by Linstead cyclization[17] of alkylated diaminomaleonitrile (DAMN), but DAMN itself fails to undergo macrocyclization. The preparation of unsubstituted amino-pz's had been unsuccessful reactions until Ercolani et al. reported the in situ generation of octaaminoporphyrazine via cyclization of 3,4-dicyano-1,2,5-selenodiazole (DCSD) to form the tetrakis(selenodiazole) porphyrazine and deprotection with H_2S, as proved by subsequent reaction with benzil to generate tetrakis(pyrazino)porphyrazine.[15] This enabled us to develop Scheme 1 for the generation of Schiff base pz's through mixed Linstead macrocyclizations of DCSD to form the soluble

(16) Mani, N. S.; Beall, L. S.; Miller, T.; Anderson, O. P.; Hope, H.; Parekin, S. R.; Williams, D. J.; Barrett, A. G. M.; Hoffman, B. M. *J. Chem. Soc., Chem. Commun.* **1994**, *18*, 2095−2096.
(17) Linstead, R. P.; Whalley, M. *J. Chem. Soc. (London)*, **1952**, 4839−4844.

Scheme 1. Synthesis of M¹[pz]−M²[Schiff Base] Complexes via 2H[pz]−M²[Schiff Base] Intermediate

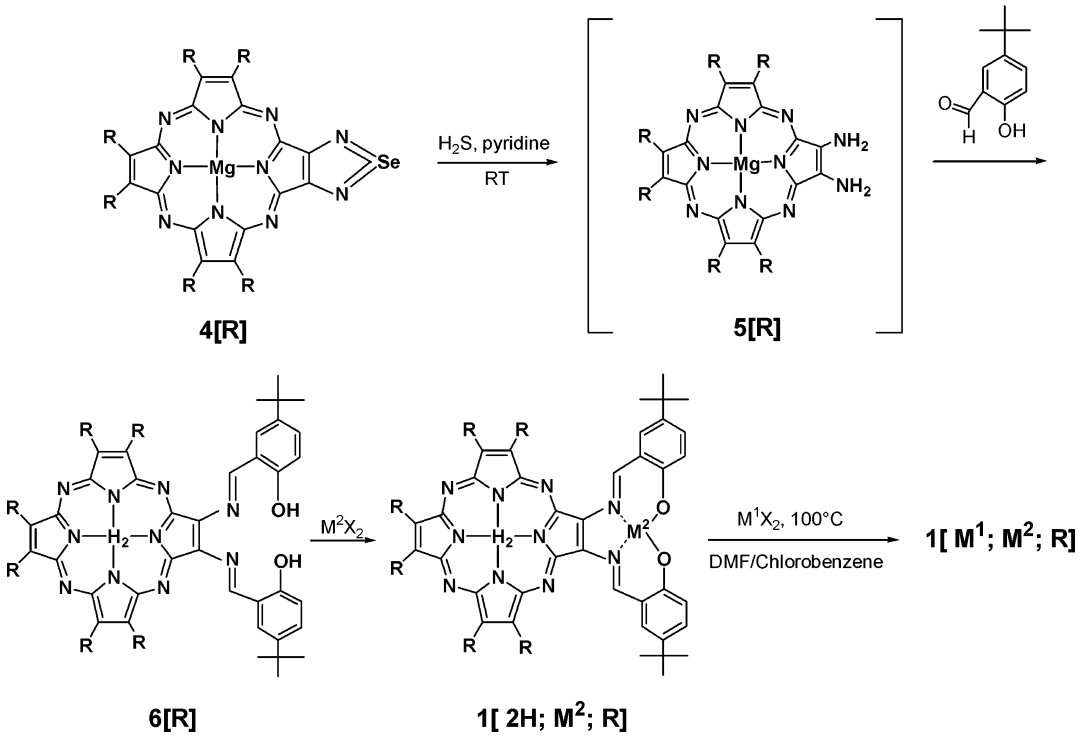

porphyrazine intermediate **4**[Pr] in 42% yield.[14] When **4**[Pr] is reductively deselenated using the conditions described by Ercolani and co-workers (H_2S, pyridine)[15] in the presence of 50-fold 5-*tert*-butyl-2-hydroxybenzaldehyde, one obtains the novel, 2H[pz]−2H[Schiff base] ligand **6**[Pr], presumably via diamine **5**[Pr]. Compound **6**[Pr] is unstable in air and could not be characterized by NMR, but its presence as an intermediate was established by MS spectroscopy and confirmed by subjecting **6**[Pr] to sequential metalation of the periphery (M^2) and the pz core (M^1) to obtain dimetallic Schiff base pz's **1**[M^1; M^2; Pr]; complexes prepared in this way are listed in Table 1.

In general, the insertion of M^1 into the pz core as the last step of Scheme 1 needs high temperature and a long reaction time, and this unfortunately tends to degrade even the most robust precursor, for example, **1**[2H; Ni; Pr]. Moreover, the process is not totally selective. M^2 incorporation into the Schiff base is difficult to control, and the pz core can be partially metalated by M^2; alternatively, M^1 sometimes can replace M^2 at high temperature.

To improve selectivity and yields, we devised an alternate synthetic approach, one which is often superior and in which the M¹[pz]−2H[Schiff base] **9**[M^1; R] is an intermediate (Scheme 2): **4**[R] is demetalated to form **7**[R], and M^1 is incorporated to form **8**[M^1; R]; subsequent deprotection and reaction with 5-*tert*-butyl-2-hydroxybenzaldehyde gives **9**[M^1; R], which can bind a metal ion to form the desired dimetallic Schiff base pz's **1**[M^1; M^2; R]. Complexes prepared in this fashion are noted in Table 1.

New Solubilizing B Group. Typically, the preparation of Schiff base pz's that employ R = *n*-propyl solubilizing group (e.g., **1**[Ni; Ni; Pr] and **1**[ClMn; Cu; Pr]) is straightforward and satisfactory. However, these complexes are not always sufficiently soluble in organic solvents for extensive physical studies. To improve the solubility of the Schiff base pz's, we developed 3,4-bis(3,4,5-trimethoxyphenyl)pyrroline-2,5-diimine, **3**, as a cyclization partner of DCSD (Scheme 3). Reaction of 3,4,5-trimethoxyphenylacetonitrile with sodium methoxide and iodine using Linstead's procedure for the oxidative coupling of substituted acetonitriles[18] yields bis-(3,4,5-trimethoxyphenyl) fumaronitrile, **2**, which is converted [19,20] to the corresponding pyrrolinediimine, **3**. Cyclization of **3** with 1 equiv of DCSD gives **4**[TMP] in ∼14% yield. In the present study, this approach has been essential for obtaining EPR spectra of a M^1 = Cu(II) and M^2 = ClMn(III) complex (Table 1).

M¹[pz]−M²[Schiff Base] Complexes. Through the use of the two synthetic schemes, we have prepared Schiff base pz's with the metal−ion pairs listed in Table 1. The 2H[pz]−Ni(II)[Schiff base] complex **1**[2H; Ni; Pr] was prepared through Scheme 1 by reaction of **6**[Pr] at room temperature with $NiCl_2$; a high temperature (100 °C) is needed for incorporation of Ni(II) into the pz core. Dark blue, needlelike crystals of **1**[2H; Ni; Pr] were grown from toluene/methanol solution. The structure is shown in Figure 1. As expected, the nickel(II) ion was coordinated to the tetradentate Schiff base site, which confirms our presumption that the peripheral coordination site binds metal ions more readily than does the pz core. However, there is extra electron density inside the pz core in excess of that for two hydrogen atoms, and this has been fitted to a partial occupancy of Ni(II) (7%). The coordination environment of the nickel ion of the Schiff base is essentially planar; the bonds to the O atoms are nearly

(18) Cook, A. H.; Linstead, R. P. *J. Chem. Soc.* **1937**, 929−933.
(19) Degener, E.; Petersen, S. U.S. Patent 2,991,292, July 4, 1961.
(20) Degener, E. *Chem. Abstr.* **1961**, *55*, 26465i.

Scheme 2. Synthesis of M^1[pz]−M^2[Schiff Base] Complexes via M^1[pz]−2H[Schiff Base] Intermediate

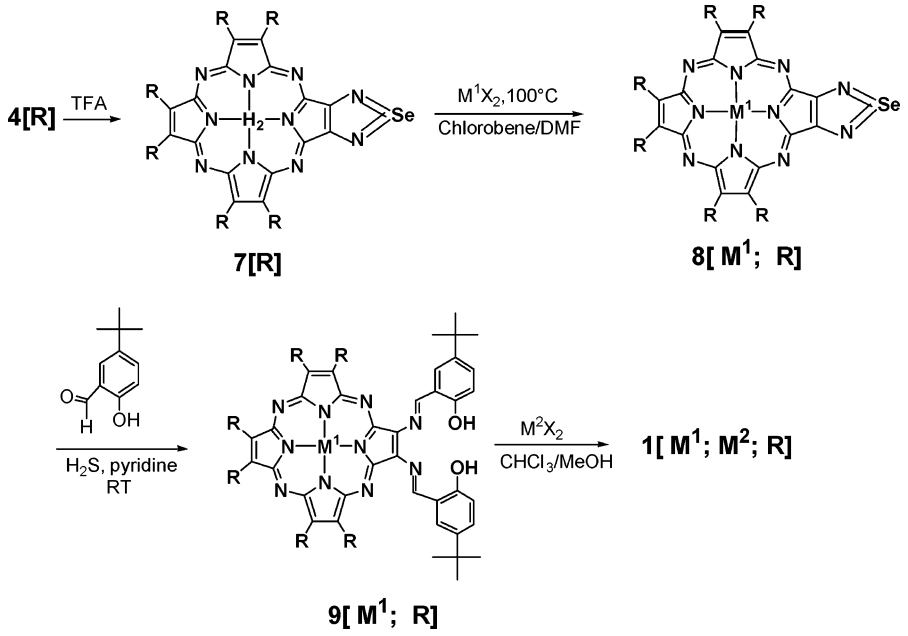

Scheme 3. Synthesis of a Cyclization Partner with New Solubilizing **B** Group: $(3,4,5\text{-Trimethoxyphenyl})_2$, $(TMP)_2$

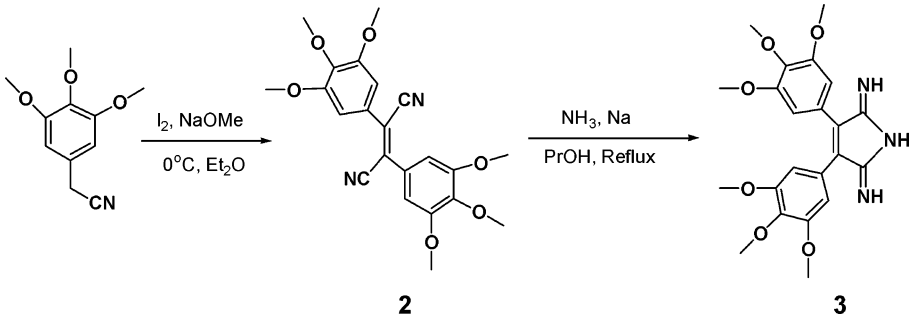

equal in length, with an average value (1.836 Å) that is slightly shorter than those to N atoms (average value, 1.871 Å).

Compound **1**[2H; Ni; Pr] was actually prepared for use as an intermediate in the preparation of M^1[pz]−M^2[Schiff base] complexes by Scheme 1, and reaction of **1**[2H; Ni; Pr] with $NiBr_2$ gives **1**[Ni; Ni; Pr]. For comparison of the two schemes, **1**[Ni; Ni; Pr] was also prepared by Scheme 2. In this case, Scheme 2 gave lower yield (20.2%, while it is 33.1% in Scheme 1), in part because **8**[Ni; Pr] is poorly soluble, which prevents its complete deselenation.

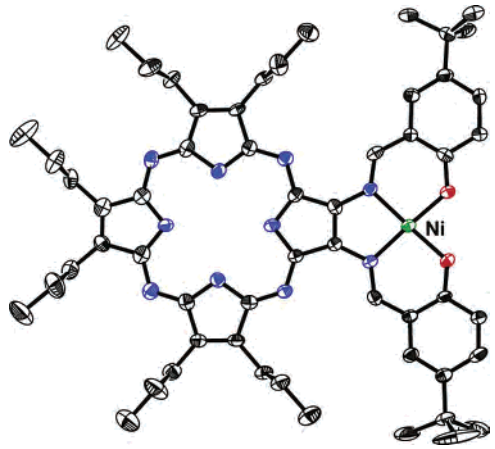

Figure 1. X-ray structure of **1**[2H; Ni; Pr].

Attempts to synthesize the intermediate 2H[pz]−Cu(II)[Schiff base] in a pure form by Scheme 1 were unsuccessful, as Cu(II) is incorporated into the pz core more readily than Ni(II). A mixture of mono- and di-copper porphyrazines is obtained, but these have similar polarities and could not be separated. However, reaction of this mixture with excess $MnCl_2$ affords **1**[ClMn; Cu; Pr], which is quite soluble in common organic solvents; as it is much more polar than other pz's in the reaction mixture, it is easily purified by column chromatography. Nonetheless, in this case, Scheme 2, with sequential core insertion of ClMn(III) followed by peripheral insertion of Cu(II), is a more efficient route to **1**[ClMn; Cu; Pr] with a yield of 40.9% compared to 30.3% by Scheme 1. The analogous compound **1**[ClMn; Ni; Pr] was prepared by Scheme 2 in the same way. The structure of **1**[ClMn; Cu; Pr], which was reported previously,[13] is shown in Figure 2.

To "switch" the place of the ClMn and Cu ion centers, **1**[Cu; ClMn; Pr] was prepared by Scheme 2, with core insertion of Cu(II) and subsequent peripheral insertion of ClMn(III). Blue, platelike crystals were grown from [toluene + CH_2Cl_2(1:1)]/CH_3CN, and Figure 2 shows the X-ray structure. The Cu(II) ion of the pz core adopts an essentially

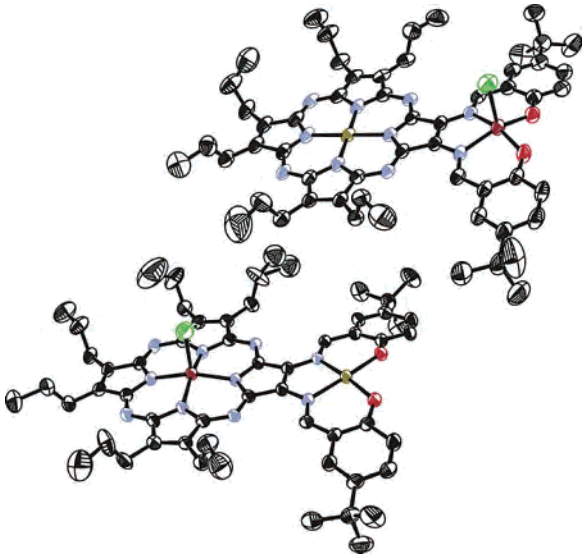

Figure 2. M^1-M^2 "isomers": X-ray structure of **1**[Cu; ClMn; Pr] (on the top) and **1**[ClMn; Cu; Pr] (on the bottom).

square-planar coordination geometry, with Cu−N bond lengths between 1.912(3) and 1.936(3) Å and N−Cu−N angles between 89.3° and 90.6°. As in a simple Mn(III) tetradentate Schiff base complex with the saltmen^{2-} ligand,[21] the Mn(III) atom of the Schiff base in **1**[Cu; ClMn; Pr] assumes a distorted square-pyramidal geometry, in which the Mn−O bonds are shorter than Mn−N by 0.149 Å, and where the apical site is occupied by the chloride anion with Mn−Cl 2.3530(14) Å.

However, insertion of square planar metal ions (e.g., Cu(II), Ni(II)) into the pz core reduces the solubility of the resulting dimetallic complexes. As a result, **1**[Cu; ClMn; Pr] is insufficiently soluble for the physical studies in solution. This case led us to develop the new **B** group, with R = TMP: **1**[Cu; ClMn; TMP] was prepared via Scheme 2, using the same strategy as **1**[Cu; ClMn; Pr], and it is soluble in most organic solvents.

UV−Vis Absorption Spectroscopy. The core atoms of the pz's discussed here have less than 4-fold symmetry and as expected display split Q-bands near 700 nm, as well as Soret bands near 350 nm.[12] In addition, **8**[Cu; Pr] and **8**[Ni; Pr] have split Soret bands which is unusual, and suggests appreciable conjugation with the selenodiazole ring. In compounds **1**[M^1; M^2; R], peripheral metalation does not cause the Q-band to coalesce to a single peak, unlike the previously reported coalesce upon peripheral metalation of dithiolato-pz's with Ni, Pt, and Pd cis-diphosphine units,[7] and with $Mo(Cp)_2$.[8] This may be due to an extension of conjugated systems on the heteroatoms in the Schiff base pz's, which is not the case in those compounds. Also, the expanded conjugated system results in a red-shifted Q-band compared with corresponding starting selenodiazole pz's **8**[M^1; R].

Electrochemistry. Cyclic voltammograms of selected pz's in dichloromethane are shown in Figure 3, and the data are

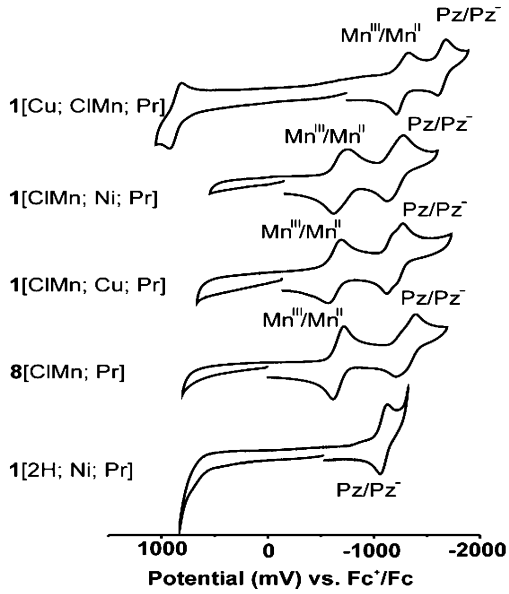

Figure 3. Cyclic voltammograms for selective pz's in CH_2Cl_2 with 0.1 M Bu_4NPF_6, referenced versus Fc^+/Fc.

Table 3. Electrochemical Data

	oxidation $E_{1/2}$/V(ΔE_p/mV)	Mn^{III}/Mn^{II} $E_{1/2}$/V(ΔE_p/mV)	Pz/Pz^- $E_{1/2}$/V(ΔE_p/mV)
1[2H; Ni; Pr]			−1.094 (58)
1[ClMn; Cu; Pr]		−0.670 (104)	−1.310 (188)
8[ClMn; Pr]		−0.654 (126)	−1.208 (150)
1[ClMn; Ni; Pr]		−0.697 (132)	−1.210 (154)
1[Cu; ClMn; Pr]	0.869 (109)	−1.275 (114)	−1.648 (76)
Mn(salen)Cl		−1.0 to −1.1	
$Mn^{II}Pc$		−0.4 to −0.5	
Mn(TPP)(Cl)(H_2O)		−0.5 to −0.7	

summarized in Table 3, together with literature values for some related compounds. A typical pz shows one or two reduction/oxidation waves for the macrocycle in addition to metal related redox waves.[12] Compound **1**[2H; Ni; Pr] shows only one reversible ring reduction at $E_{1/2} = -1094$ mV (Pz^-/Pz) (all potentials referred to Fc^+/Fc; see Experimental Section) and no ring oxidation within the solvent range. The Mn^{III}/Mn^{II} reduction waves for manganese(III) pz's **8**[ClMn; Pr], **1**[ClMn; Cu; Pr], and **1**[ClMn; Ni; Pr] occur at about −0.67 V, which are comparable with literature values for other Mn macrocycles: the Mn^{III}/Mn^{II} couple has a potential of −0.4 to −0.5 V for $Mn^{II}Pc$,[22,23] while for related tetraphenylporphyrin compounds, the analogous half-wave potential lies between ca. −0.5 and −0.7 V.[24,25] The second reversible reductions are assigned to the Pz/Pz^- ring reduction. This redox couple of **8**[ClMn; Pr] (- 1.310 V) is about 100 mV more negative than that of **1**[ClMn; Cu; Pr] (−1.208 V), and **1**[ClMn; Ni; Pr] (−1.210 V), which suggests that the selenodiazole ring is a stronger electron withdrawing group than the Schiff base complexes, which makes the reduction of the pz ring more difficult. For compound **1**[Cu; ClMn; Pr], the Mn^{III}/Mn^{II} reduction wave centers at −1.275

(21) Miyasaka, H.; Clerac, R.; Ishii, T.; Chang, H. C.; Kitagawa, S.; Yamashita, M. *J. Chem. Soc., Dalton Trans.* **2002**, 1528−1534.

(22) Lever, A. B. P.; Minor, P. C.; Wilshire, J. P. *Inorg. Chem.* **1981**, *20*, 2550−2553.

(23) Lever, A. B. P.; Pickens, S. R.; Minor, P. C.; Licoccia, S.; Ramaswamy, B. S.; Magnell, K. *J. Am. Chem. Soc.* **1981**, *103*, 6800−6806.

(24) Boucher, L. J. *Coord. Chem. Rev.* **1972**, *7*, 289−329.

(25) Boucher, L. J.; Garber, H. K. *Inorg. Chem.* **1970**, *9*, 2644−2649.

V. This value can be comparable to those of Mn^{III}(salen)Cl and related Schiff base compounds, which fall between −1.0 and −1.1 V,[26] and is about 500 mV more negative than that of Mn^{III} in the pz core. A quasireversible wave at 0.869 V could represent either the Mn^{IV}/Mn^{III} oxidation[26−29] or pz ligand-centered oxidation.[12]

Magnetic Properties. First we discuss the properties of individual paramagnetic metal ions at the core and periphery, and then those of the two "isomers" of the dimetallic **1**[M^1; M^2; R] formed with ClMn(III) and Cu(II).

ClMn(III) and Cu(II) Sites. High-field EPR measurements showed that a Mn(III) ion incorporated in a ClMn(III) pz has a high-spin ($S = 2$), d^4 configuration; an axial zero-field splitting (zfs) interaction resolves the four $S = 2$ spin sublevels into ±1/2 and ±3/2 doublets that are separated in zero field by $2D^{Mn} = -4.6$ cm^{-1} ($E^{Mn} = 0$), which is far greater than the X-band microwave quantum.[30] As a result, monometallic pz's with ClMn(III), such as compound **8**[ClMn; Pr], give no X-band signal. A ClMn(III) in a N_2O_2 tetradentate Schiff base complex also is high-spin ($3d^4$, $S = 2$), and high-field EPR frozen solution spectra yield $D = -2.47$ cm^{-1}; the reduced symmetry of the N_2O_2 coordination environment introduces a rhombic zero-field splitting component.[31]

The EPR spectrum at 77 K of a powder sample of 1% **8**[Cu; Pr] magnetically diluted in its diamagnetic host **7**[Pr] has the axial symmetry typical for monomeric square-planar Cu(II) complexes: $g_\perp = 2.05$, $g_\parallel = 2.14$, $A_\parallel^{Cu} = 220.0$ G. In addition, the spectrum shows well-resolved ^{14}N hyperfine coupling from the coordinated nitrogen atoms, with a splitting $B_N = 16.0$ G for the field normal to the Cu−N bond. A nine-line splitting in the $g_\perp$ region corresponds to the average, $(A_N + B_N)/2$, where A_N is the coupling along the Cu−N bond, and gives $A_N = 17.5$ G. Compound **8**[Cu; TMP] shows a similar frozen solution EPR spectrum, with similar parameters. The g values and hyperfine constants are close to those of other copper porphyrazines.[6,7,32]

The d^9 Cu(II) ion in an isolated Schiff base compound has $S = 1/2$ and behaves quite similarly, with $g_\parallel \approx 2.2$, $g_\perp \approx 2.05$, and $A_\parallel^{Cu} \approx 197$ G.[33]

Spin-Coupled ClMn(III) and Cu(II). Figure 4 displays X-band EPR spectra of **1**[ClMn; Cu; Pr] and **1**[Cu; ClMn; TMP] taken at 77 K. It was impossible to obtain a frozen-solution EPR spectrum of **1**[Cu; ClMn; Pr] because of poor solubility, but the solubility of **1**[Cu; ClMn; TMP] is more than adequate to allow us to collect its X-band EPR spectrum.

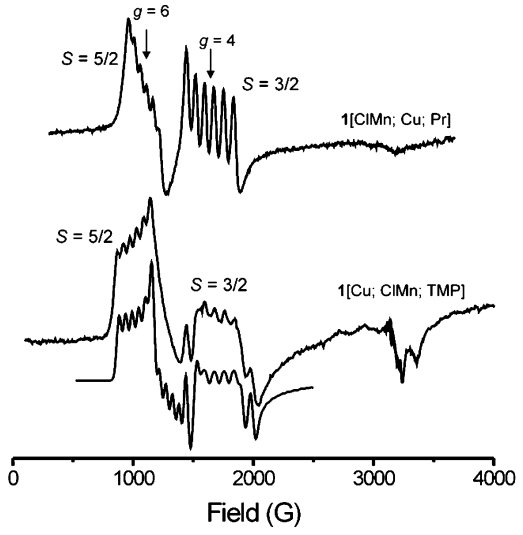

Figure 4. X-band EPR of **1**[ClMn; Cu; Pr] in toluene/pyridine (1:1) and **1**[Cu; ClMn; TMP] (with simulation below) in $CH_2Cl_2/CHCl_3$ (9:1) at 77 K.

Both spectra show "perpendicular" features at $g_\perp \sim 6$ and $g_\perp \sim 4$, the former characteristic of a $S = 5/2$ spin state, the latter of a $S = 3/2$ state, both with an axial zero-field splitting (zfs) parameter (D^S) that is large compared to the microwave quantum;[34] the spectrum of **1**[Cu; ClMn; TMP] further shows a rhombic splitting of both $g_\perp \sim 4$ and $g_\perp \sim 6$ features. Each of the spectra displays sextet splittings from interaction with ^{55}Mn($I = 5/2$). The spectrum of **1**[ClMn; Cu; Pr] further shows unresolved intensity from the associated $g_\parallel$ features around $g = 2$; that from **1**[Cu; ClMn; TMP] must do so as well, but the region is partially obscured by a signal from residual **1**[Cu; 2H; TMP].

These spectra are the result of strong Heisenberg exchange coupling between the $S = 2$ and $S = 1/2$ individual spins. The exchange Hamiltonian, $\hat{H}_{ex} = JS_1 \cdot S_2$, produces two total-spin manifolds with $S = 3/2$ and $5/2$, separated by $\Delta = 5J$. Each of the $S = 3/2$ and $5/2$ manifolds exhibits an axial zfs interaction whose principal value (D^S) is determined by that of the uncoupled Mn(III) ion: $D^{3/2} = (3/5)D^{Mn}$; $D^{5/2} = (7/5)D^{Mn}$; the same numerical factors scale E^{Mn} to give $E^{3/2}$ and $E^{5/2}$. For both M^1-M^2 isomers, the D^S ($S = 3/2, 5/2$) values are much larger than the X-band microwave quantum, and the X-band spectra display only transitions within the $m_s = \pm 1/2$ doublet for each total-spin manifold. For **1**[ClMn; Cu; Pr], the $S = 5/2$ and $3/2$ g tensors both are axial, corresponding to $E^{Mn} = 0$: $g_\perp^{3/2} = 4$, $g_\perp^{5/2} = 6$, and $g_\parallel^{3/2} = g_\parallel^{5/2} = 2$. In the exchange-coupled system, $A_{Mn}^{3/2} = (6/5)A_{Mn}$ and $A_{Mn}^{5/2} = (4/5)A_{Mn}$, where A_{Mn} is the coupling for the isolated Mn(III). The resulting prediction that $A_{Mn}^{3/2}/A_{Mn}^{5/2} = 3/2$ matches the observed ratio of couplings for **1**[ClMn; Cu; Pr], $A_{Mn}^{3/2}/A_{Mn}^{5/2} = 80\text{G}/53\text{ G} = 1.51$; the resulting hyperfine interaction for the uncoupled Mn(III), $A_{Mn} = 66$ G, is typical for such ions.[35] The absence of hyperfine splittings by the $^{63/65}$Cu also is

(26) Hirotsu, M.; Nakajima, K.; Kojima, M.; Yoshikawa, Y. *Inorg. Chem.* **1995**, *34*, 6173−6178.
(27) Panja, A.; Shaikh, N.; Butcher, R. J.; Banerjee, P. *Inorg. Chim. Acta* **2003**, *351*, 27−33.
(28) Hoyos, O. L.; Bermejo, M. R.; Fondo, M.; Garcia-Deibe, A.; Gonzalez, A. M.; Maneiro, M. B.; Pedrido, R. *J. Chem. Soc., Dalton Trans.* **2000**, 3122−3127.
(29) Bermejo, M. R.; Gonzalez, A. M.; Fondo, M.; Garcia-Deibe, A.; Maneiro, M.; Sanmartin, J.; Hoyos, O. L.; Watkinson, M. *New J. Chem.* **2000**, *24*, 235−241.
(30) Krzystek, J.; Telser, J.; Pardi, L. A.; Goldberg, D. P.; Hoffman, B. M.; Brunel, L.-C. *Inorg. Chem.* **1999**, *38*, 6121−6129.
(31) Krzystek, J.; Telser, J. *J. Magn. Reson.* **2003**, *162*, 454−465.
(32) Schramm, C. J.; Hoffman, B. M. *Inorg. Chem.* **1980**, *19*, 383−385.
(33) Tauber, C. E.; Allen, H. C., Jr. *J. Phys. Chem.* **1979**, *83*, 1391−1393.
(34) Weltner, W., Jr. In *Magnetic Atoms and Molecules*; Dover: New York, 1983; pp 266−277.
(35) Peloquin, J. M.; Campbell, K. A.; Randall, D. W.; Evanchik, M. A.; Pecoraro, V. L.; Armstrong, W. H.; Britt, R. D. *J. Am. Chem. Soc.* **2000**, *122*, 10926−10942.

explained by the exchange model. Calculations show[13] that the copper hyperfine coupling is sharply reduced in the total-spin manifolds generated by the spin exchange: $A_\perp(\mathrm{Cu})^{3/2} = A_\perp(\mathrm{Cu})^{5/2} = \pm(^1/_5)A_\perp(\mathrm{Cu})$. The observation of both signals at 77 K implies a thermal population of the two spin manifolds at this temperature. In spectra taken at lower temperature, the $S = {}^5/_2$ signal decreases in intensity relative to the $S = {}^3/_2$ signal, indicative antiferromagnetic coupling, $J > 0$.

The EPR spectra for both the $S = {}^5/_2$ and the $S = {}^3/_2$ spin states of compound **1**[Cu; ClMn; TMP] exhibit a rhombic **g**-splitting: simulations give $g_1{}^{5/2} = 6.45$ ($A^{5/2} = 55$ G), $g_2{}^{5/2} = 5.00$ ($A^{5/2} = 55$ G); $g_1{}^{3/2} = 3.638$ ($A^{3/2} = 82.5$ G), $g_2{}^{3/2} = 3.968$ ($A^{3/2} = 82.5$ G) (Figure 4). The ratio $A_{\mathrm{Mn}}{}^{5/2}/A_{\mathrm{Mn}}{}^{3/2} = 82.5$ G/55 G $= 1.5$, which again matches the theoretical value, $^3/_2$. The $g_\perp$ feature splits because of the rhombic zfs of the Mn(III) ion in the Schiff base.[31] Although the rhombicity in g is larger for the $S = {}^5/_2$ state, $\delta g^{5/2} = (g_1{}^{5/2} - g_2{}^{5/2}) = 1.45$, while $\delta g^{3/2} = (g_1{}^{3/2} - g_2{}^{3/2}) = 0.33$, it can be shown that the two g tensors are internally consistent, with $|E^{\mathrm{Mn}}/D^{\mathrm{Mn}}| = |E^{5/2}/D^{5/2}| = |E^{3/2}/D^{3/2}| \approx 0.09$, in satisfactory agreement with the high-field EPR measurement, which gave $|E^{\mathrm{Mn}}/D^{\mathrm{Mn}}| = 0.07$.[31]

The detailed analysis of the spectra in Figure 4 shows definitively that **1**[ClMn; Cu; R] and **1**[Cu; ClMn; R] exhibit strong Heisenberg spin exchange between the partner metal−ion spins, and the temperature dependence of the ratio of $S = {}^3/_2$ and $S = {}^5/_2$ signals indicates that the exchange parameter, Δ, that splits the $S = {}^3/_2$ and $S = {}^5/_2$ manifolds is positive for both. It is not a priori clear whether Δ should be the same for the two molecules: Mn(III) can participate in π-bonding, while Cu(II) cannot; the pz ring might be better suited for π-bonding than the Schiff base chelate, thereby delocalizing spin toward the periphery for $\sigma-\pi$ coupling to the Cu(II). It is possible to determine Δ by analysis of the temperature dependence of EPR intensities, but it is more accurate to measure the magnetic susceptibility. This was done for both compounds over the temperature range 2−300 K using a SQUID magnetometer (Figure 5). Both compounds exhibit a high-temperature limiting value, $\chi T \sim 3.5$ $\mathrm{cm^3 mol^{-1} K}$, consistent with the presence of $S = 2$ and $S = {}^1/_2$ partner spins, each having intrinsic g values of roughly 2.

The measured $\chi(T)$ was fit to the theoretical expression, eq 1[36]

$$\chi = \chi^{3/2}\frac{2}{2+3\mathrm{e}^{-\Delta/k_\mathrm{B}T}} + (C/4)\frac{35\mathrm{e}^{-\Delta/k_\mathrm{B}T}}{2+3\mathrm{e}^{-\Delta/k_\mathrm{B}T}}$$

$$\chi^{3/2} = C\left[\frac{1}{3}\frac{1+9\mathrm{e}^{-2D^{3/2}/k_\mathrm{B}T}}{4(1+\mathrm{e}^{-2D^{3/2}/k_\mathrm{B}T})} + \frac{2}{3}\frac{4+\dfrac{3k_\mathrm{B}T}{D^{3/2}}(1-\mathrm{e}^{-2D^{3/2}/k_\mathrm{B}T})}{4\,(1+\mathrm{e}^{-2D^{3/2}/k_\mathrm{B}T})}\right] \quad (1)$$

where $C = N\mu_\mathrm{B}{}^2 g^2/k_\mathrm{B}(T-\theta)$ and the symbols have their usual meanings. The function $\chi^{3/2}$ is associated with the $S = {}^3/_2$ manifold and incorporates the effects of the zero-field splitting: $D^{3/2} = (^3/_5)D^{\mathrm{Mn}}$, where $D^{\mathrm{Mn}} = -2.3$ $\mathrm{cm^{-1}}$ for **1**[ClMn; Cu; R],[30] and $D^{\mathrm{Mn}} = -2.47$ $\mathrm{cm^{-1}}$ for **1**[Cu; ClMn; R].[31] The fits give $\Delta/k_\mathrm{B} = 23$ K and the Curie−Weiss constant, $\theta = -8$ K for **1**[ClMn; Cu; Pr], and $\Delta/k_\mathrm{B} = 20.4$ K, $\theta = -0.36$ K for **1**[Cu; ClMn; Pr]. The equivalent values of Δ for the two $\mathrm{M^1}-\mathrm{M^2}$ "isomers" indicate that σ-delocalization dominates, with little contribution from a pathway involving π-delocalization from Mn(III) and exchange-polarization coupling to Cu(II).

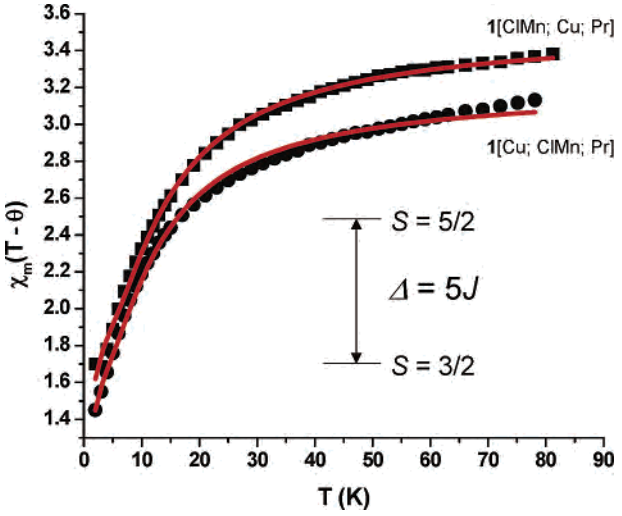

Figure 5. Plot of the molar magnetic susceptibility of a powdered sample of **1**[ClMn; Cu; Pr] (■) and **1**[Cu; ClMn; Pr] (●) plotted as (χT), which corresponds to the effective moment squared. The solid line is a fit to the data by eq 1, with $\theta = -8$ K, $g = 2.05$, $D^{3/2} = (^3/_5)D^{\mathrm{Mn}} = -1.38$ $\mathrm{cm^{-1}}$, and $\Delta/k_\mathrm{B} = 23$ K for **1**[ClMn; Cu; Pr]; and with $\theta = -0.36$ K, $g = 1.95$, $D^{3/2} = (^3/_5)D^{\mathrm{Mn}} = -1.482$ $\mathrm{cm^{-1}}$, and $\Delta/k_\mathrm{B} = 20.4$ K for **1**[Cu; ClMn; Pr].

Conclusion

We have devised two alternate schemes for the preparation of Schiff base porphyrazines, developed a new solubilizing group to aid in their study, and prepared a series of these pz's. X-ray structures have been determined for 2H[pz]−Ni(II)[Schiff base], **1**[2H; Ni; Pr], and Cu(II)[pz]−ClMn(III)[Schiff base], **1**[Cu; ClMn; Pr]. The metal ions of the $\mathrm{M^1}-\mathrm{M^2}$ "isomers", **1**[ClMn; Cu; R] and **1**[Cu; ClMn; R], are exchange-coupled and exhibit EPR spectra which are the superposition of signals from $S = {}^5/_2$ and $S = {}^3/_2$ total-spin manifolds. The exchange splitting between manifolds is essentially the same in the two isomers, which suggests a purely σ-pathway for exchange coupling.

Acknowledgment. This work has been supported by the NSF (Grant CHE-0091364, B.M.H.) and the EPSRC (A.G.M.B.), and through the NU Materials Research Center (DMR-0076097). The authors also would like to thank Dr. Roman M. Davydov and Dr. Peter E. Doan for low temperature EPR measurements and helpful discussions.

Supporting Information Available: CIF files for the compounds **1**[2H; Ni; Pr] and **1**[Cu; ClMn; Pr]. These materials are available free of charge via the Internet at http://pubs.acs.org.

IC035402X

(36) O'Connor, C. J. *Prog. Inorg. Chem.* **1982**, *29*, 203−283.